JACC: CARDIOVASCULAR IMAGING VOL. 14, NO. 8, 2021

ORIGINAL RESEARCH

Myocardial Fibrosis and Inflammation by CMR Predict Cardiovascular Outcome in People Living With HIV

Philipp de Leuw, MD,[a,b,*] Christophe T. Arendt, MD,[c,d,*] Annette E. Haberl, MD,[a] Daniel Froadinadl, MED,[a] Gerrit Kann, MD,[a] Timo Wolf, MD,[a] Christoph Stephan, MD,[a] Gundolf Schuettfort, MD,[a] Moises Vasquez, MD,[c,e] Luca Arcari, MD,[c,f] Hui Zhou, MD,[c,g] Hafisyatul Zainal, MD,[c,h] Monika Gawor, MD,[c,i] Eleftherios Vidalakis, MD,[c] Michael Kolentinis, MD,[c] Moritz H. Albrecht, MD,[c,d] Felicitas Escher, MD,[j] Thomas J. Vogl, MD,[d] Andreas M. Zeiher, MD,[k] Eike Nagel, MD,[c] Valentina O. Puntmann, PhD[c,i]

ABSTRACT

OBJECTIVES The goal of this study was to examine prognostic relationships between cardiac imaging measures and cardiovascular outcome in people living with human immunodeficiency virus (HIV) (PLWH) on highly active antiretroviral therapy (HAART).

BACKGROUND PLWH have a higher prevalence of cardiovascular disease and heart failure (HF) compared with the noninfected population. The pathophysiological drivers of myocardial dysfunction and worse cardiovascular outcome in HIV remain poorly understood.

METHODS This prospective observational longitudinal study included consecutive PLWH on long-term HAART undergoing cardiac magnetic resonance (CMR) examination for assessment of myocardial volumes and function, T1 and T2 mapping, perfusion, and scar. Time-to-event analysis was performed from the index CMR examination to the first single event per patient. The primary endpoint was an adjudicated adverse cardiovascular event (cardiovascular mortality, nonfatal acute coronary syndrome, an appropriate device discharge, or a documented HF hospitalization).

RESULTS A total of 156 participants (62% male; age [median, interquartile range]: 50 years [42 to 57 years]) were included. During a median follow-up of 13 months (9 to 19 months), 24 events were observed (4 HF deaths, 1 sudden cardiac death, 2 nonfatal acute myocardial infarction, 1 appropriate device discharge, and 16 HF hospitalizations). Patients with events had higher native T1 (median [interquartile range]: 1,149 ms [1,115 to 1,163 ms] vs. 1,110 ms [1,075 to 1,138 ms]); native T2 (40 ms [38 to 41 ms] vs. 37 ms [36 to 39 ms]); left ventricular (LV) mass index (65 g/m^2 [49 to 77 g/m^2] vs. 57 g/m^2 [49 to 64 g/m^2]), and N-terminal pro-B-type natriuretic peptide (109 pg/l [25 to 337 pg/l] vs. 48 pg/l [23 to 82 pg/l]) (all $p < 0.05$). In multivariable analyses, native T1 was independently predictive of adverse events (chi-square test, 15.9; $p < 0.001$; native T1 [10 ms] hazard ratio [95% confidence interval]: 1.20 [1.08 to 1.33]; $p = 0.001$), followed by a model that also included LV mass (chi-square test, 17.1; $p < 0.001$). Traditional cardiovascular risk scores were not predictive of the adverse events.

CONCLUSIONS Our findings reveal important prognostic associations of diffuse myocardial fibrosis and LV remodeling in PLWH. These results may support development of personalized approaches to screening and early intervention to reduce the burden of HF in PLWH (International T1 Multicenter Outcome Study; NCT03749343).

ISSN 1936-878X https://doi.org/10.1016/j.jcmg.2021.01.042

People living with human immunodeficiency virus (HIV, PLWH) have an increased risk of developing cardiovascular disease compared with the noninfected population. The increased prevalence of cardiovascular disease has been traditionally attributed to the accelerated effects of traditional cardiovascular risk factors, as well as the dysmetabolic effects of the long-term highly active antiretroviral therapy (HAART) (1,2). However, studies increasingly suggest that myocardial inflammatory remodeling and fibrosis play a role in promoting the high incidence of heart failure (HF) (3). Several cardiac imaging studies provided insights into the underlying pathophysiology by revealing complex patterns of structural heart disease, including impaired systolic and diastolic function (4), reduced myocardial strain, and increased left ventricular (LV) mass and remodeling (5,6). Studies using cardiovascular magnetic resonance (CMR) also exhibited a high incidence of microvascular disease, cardiac steatosis, and higher rate and more extensive myocardial scarring.

More recently, the contribution of HIV-related chronic immune activation, dysregulation, and inflammation in driving subclinical cardiac dysfunction and HF have also been recognized (7,8). No study to date, however, has comprehensively evaluated prognostic associations of cardiac imaging measures, including native T1 and T2 mapping, or compared them versus the conventional and modified cardiovascular risk scores. We hypothesized that CMR biosignatures of diffuse myocardial remodeling and fibrosis provide predictive associations with cardiovascular outcome events.

METHODS

This study was a prospective, longitudinal, observational, investigator-led analysis of the prognostic value of T1 mapping in adult participants undergoing a clinical CMR (NCT03749343). Consecutive participants (n = 156) with an established diagnosis of HIV infection were referred from the specialist HIV Center at the University Hospital Frankfurt (Frankfurt am Main, Germany) for assessment of any heart involvement due to an inherently high risk of cardiovascular disease (9). Owing to the known high prevalence of nonischemic cardiac pathology, the presence of typical cardiac symptoms was not mandatory. The HIV specialist clinical care was provided in line with current guidelines and recommendations from the European AIDS Clinical Society (10), independently of the cardiac imaging research team. Exclusion criteria were contraindications to CMR such as magnetic resonance–unsafe implantable devices (n = 0), history of previous allergic reaction to gadolinium-based contrast agent (n = 1), and inability to provide informed consent (n = 2). An eGRF <30 ml/min/1.73 m^2 was not a contraindication, in line with current recommendations for diagnostic use of gadolinium-based contrast agents (11).

The study protocol was reviewed and approved by the institutional ethics committee, and written informed consent was obtained from all participants. All procedures were performed in accordance with the Declaration of Helsinki (2013). Systematic risk scores for cardiovascular disease (Framingham Risk Score of coronary artery disease [12], the Data Collection on Adverse Effects of Anti-HIV Drugs [D:A:D] score [13], and the Meta-Analysis Global Group in Chronic Heart Failure [MAGGIC] integer score [14]) were calculated by using original online calculators.

IMAGING PROCEDURES. Participants underwent a standardized CMR imaging protocol using a 3.0-T

ABBREVIATIONS AND ACRONYMS

CI = confidence interval

CMR = cardiac magnetic resonance

D:A:D = Data Collection on Adverse Effects of Anti-HIV Drugs

HAART = highly active antiretroviral therapy

HF = heart failure

HIV = human immunodeficiency virus

HR = hazard ratio

hs-TnT = high-sensitivity troponin T

IQR = interquartile range

LV = left ventricular

LGE = late gadolinium enhancement

MAGGIC = Meta-Analysis Global Group in Chronic Heart Failure Risk Score

MOLLI = modified Look-Locker imaging

NT-proBNP = N-terminal pro-B-type natriuretic peptide

PLWH = people living with human immunodeficiency virus

From the [a]HIV Center, Department of Infectious Diseases, University Hospital Frankfurt, Frankfurt am Main, Germany; [b]Infektiologikum, Frankfurt am Main, Germany; [c]Institute of Experimental and Translational Cardiac Imaging, DZHK (German Centre for Cardiovascular Research) Centre for Cardiovascular Imaging, University Hospital Frankfurt, Frankfurt am Main, Germany; [d]Department of Diagnostic and Interventional Radiology, University Hospital Frankfurt, Frankfurt am Main, Germany; [e]Cardiology Department, Enrique Baltodano Briceño Hospital, Liberia, Costa Rica; [f]Department of Cardiology, School of Medicine and Psychology, Sapienza University of Rome, Rome, Italy; [g]Department of Radiology, XiangYa Hospital, Central South University, Changsha, Hunan, China; [h]Department of Cardiology, Universiti Teknologi MARA (UiTM), Sg. Buloh, Malaysia; [i]Department of Cardiology, University Hospital Warsaw, Warsaw, Poland; [j]Institute for Cardiac Diagnostic and Therapy, Berlin, Germany; and the [k]Department of Cardiology, University Hospital Frankfurt, Frankfurt am Main, Germany. *Drs. de Leuw and Arendt contributed equally to this work and are joint first authors.

Tim Leiner, MD, served as Guest Editor.

The authors attest they are in compliance with human studies committees and animal welfare regulations of the authors' institutions and Food and Drug Administration guidelines, including patient consent where appropriate. For more information, visit the Author Center.

Manuscript received September 14, 2020; revised manuscript received December 30, 2020, accepted January 28, 2021.

TABLE 1 Baseline Characteristics of the Study Participants

	No CV Events (n = 132)	CV Events (n = 24)	p Value
Age, yrs	50 (42-57)	53 (43-58)	0.15
Male	83 (63)	14 (58)	0.64
White	105 (80)	17 (71)	0.73
Cardiovascular risk factors			
Obesity (BMI >30 kg/m^2)	32 (24)	4 (17)	0.56
Arterial hypertension	29 (22)	6 (25)	0.79
Diabetes	7 (5)	1 (4)	0.64
Hypercholesterolemia	21 (16)	5 (21)	0.56
Family history of CVD	10 (8)	1 (4)	0.49
Smoking (current or previous)	46 (35)	11 (45)	0.56
Coronary artery disease	13 (10)	5 (21)	0.16
Previous revascularization	13 (10)	5 (21)	0.16
Previous myocarditis	6 (5)	1 (4)	0.86
Previous diagnosis of HF	19 (14)	4 (16)	0.73
Atrial fibrillation	4 (3)	1 (4)	0.53
Peripheral arterial disease	9 (7)	2 (8)	0.86
Previous stroke or TIA	4 (3)	0 (0)	0.65
Cardiovascular risk scores			
NYHA functional class ≥III	25 (19)	7 (29)	0.26
D:A:D (R) 5-yr risk score, %	21 (10-34)	22 (4-35)	0.16
D:A:D (F) 5-yr risk score, %	16 (9-34)	22 (4-34)	0.39
FRS 10 YRS, %	13 (7-25)	18 (11-30)	0.07
MAGGIC 1-yr risk score, %	4 (2-6)	5 (2-7)	0.16
HIV characteristics			
HIV CDC classification			
Stage A1-A3	59 (45)	12 (50)	0.71
Stage B1-B3	42 (32)	7 (29)	0.94
Stage C1-C3	31 (23)	5 (21)	0.72
HIV treatment	131 (99)	24 (100)	0.62
Protease inhibitors	34 (26)	9 (38)	0.31
NRTIs	99 (75)	21 (87)	0.29
NNRTIs	16 (12)	7 (31)	0.04
Integrase inhibitors	57 (43)	3 (13)	0.02
Fusion inhibitors	18 (14)	3 (13)	0.91
CCR5 antagonist	4 (3)	0 (0)	0.49
Post-attachment inhibitor	7 (5)	0 (0)	0.36
Hepatitis B	8 (6)	1 (4)	1.00
Hepatitis C	8 (6)	1 (4)	1.00
Syphilis	33 (25)	9 (38)	0.27

Values are median (interquartile range) or n (%). Comparison between groups was made between participants with and without events ($p < 0.05$ considered significant).

BMI = body mass index; CCR5 = C-C motif chemokine receptor 5; CDC = Centers for Disease Control and Prevention; CV = cardiovascular; CVD = cardiovascular disease; D:A:D = Data Collection on Adverse Effects of Anti-HIV Drugs; HF = heart failure; HIV = human immunodeficiency virus; NYHA = New York Heart Association; FRS = Framingham Risk Score; MAGGIC = Meta-Analysis Global Group in Chronic Heart Failure Risk Score; NRTIs = nucleoside reverse transcriptase inhibitors; NNRTIs = non-nucleoside reverse transcriptase inhibitors; TIA = transient ischemic attack.

clinical scanner (Skyra, Siemens Healthineers, Erlangen, Germany, Software Version VE11) for acquisition of cardiac function, volumes, mass, myocardial T1 and T2 maps, myocardial perfusion, and scar (15). All sequence parameters have been published previously (16-18) and are detailed in the Supplemental Appendix. Myocardial T1 and T2 mapping were acquired in a single midventricular short-axis slice by using a validated variant of a modified Look-Locker imaging (MOLLI) sequence (Goethe CVI, Frankfurt, Germany) (16-18), whereas for T2 mapping, a validated sequence for measurement of myocardial edema was used (T2-FLASH) (19,20). Due to the proven sensitivity of Goethe CVI MOLLI for abnormal myocardium and evidence of superior diagnostic and prognostic performance (16-18), post-contrast T1 mapping was not part of the standardized protocol. Myocardial perfusion imaging was performed during maximal vasodilation (regadenoson, 400 μg/5 ml) and administration of gadolinium contrast agent (0.1 mmol/kg body weight gadobutrol [Gadovist, Bayer AG, Leverkusen, Germany]). The presence of myocardial scar was visualized by late gadolinium enhancement (LGE) imaging at 7 to 10 min after administration of gadolinium-based contrast agent.

Analysis of cardiac volumes, function, and mass was performed by using semi-automated contour detection (suiteHEART, Neosoft, Pewaukee, Wisconsin). Interpretation of myocardial perfusion and LGE images was performed visually following standardized procedures for data display and image interpretation (21). Myocardial LGE was visually defined by consensus of 2 observers based on the presence/absence and the predominant pattern as ischemic or nonischemic. Quantitative tissue characterization analysis was performed by the core laboratory staff (Goethe CVI Core Lab, Frankfurt am Main, Germany), blinded to the underlying clinical information. Details of post-processing and interpretation, including the cutoff values, have been reported previously and are included in the Supplemental Appendix. Myocardial T1 and T2 relaxation times were measured by using a standardized operating procedure (ConSept study), by placing the region of interest conservatively within the septal myocardium of a midventricular short-axis slice in motion-corrected images (22,23). Areas of LGE were excluded from regions of interest to avoid mixing in the areas with replacement scar. Myocardial perfusion was evaluated visually, and the presence of significant ischemia was considered positive if 2 of 32 subsegments showed a perfusion defect during vasodilator stress (24,25). LGE was quantified by a semiautomatic detection method using full width at one-half maximum method and is reported as a percentage of the total LV mass.

BLOOD SAMPLING. Venous blood samples were taken immediately before the CMR study and processed according to standard procedures. Commercially available test kits were used for analysis of high-sensitivity troponin T (hs-TnT) and N-terminal pro-B-type natriuretic peptide (NT-proBNP) (Elecsys 2010, Roche, Basel, Switzerland) levels.

CARDIOVASCULAR OUTCOMES. Follow-ups were performed by review of electronic databases and telephone interviews, all of which were completed before December 2019. Medical records were examined for details of clinical presentations, entries of outpatient visits, hospitalizations, and medical procedures. All events were adjudicated by independent physicians, according to the established and predefined endpoint definitions (26). The primary endpoint was a composite of adverse cardiovascular events (cardiovascular mortality, nonfatal acute coronary syndrome, an appropriate device discharge, or HF hospitalization). Acute coronary syndrome was defined by a significant rise in hs-TnT in the presence of typical symptoms (27). HF hospitalization was defined by an episode of hospitalization with symptoms and signs of HF that were accompanied by a significant increase in NT-proBNP levels (26,28). An appropriate device discharge was defined as a documented shock delivered through an implanted cardioverter device that terminated a life-threatening ventricular arrhythmia (i.e., ventricular tachycardia or fibrillation) (26). The first single event per patient was included in the analysis.

STATISTICAL ANALYSIS. Analysis was performed by using SPSS software version 25.0 (IBM SPSS Statistics, IBM Corporation, Armonk, New York). All tests were two-tailed, and a p value ≤0.05 was statistically significant. Data are presented as counts (percentage) for categorical data or median (interquartile range [IQR]) for continuous variables. The Fisher exact and nonparametric tests were used to compare the groups with events and without them (Mann-Whitney *U* test). Time to-event analysis was performed from the date of the index CMR study. Univariable Cox proportional hazards models were used to examine the association between the endpoint and baseline covariates (unadjusted hazard ratio [HR] with 95% confidence interval [CI]). Multivariable analysis was performed with backward stepwise selection (Wald) modeling to determine the independent associations with the primary endpoint (adjusted HR [95% CI]); the thresholds for the backward selection process in the model included a p value of 0.05 for entry and 0.10 for removal of a variable. The rule of thumb for Cox models with a minimum of 10 outcome events per predictor variable was used. Variables with nonnormal distribution underwent log-transformation before inclusion into the Cox regression models. The final number of included subjects was ascertained by using interim power analyses for the predefined endpoints. A post hoc analysis is provided in the Supplemental Appendix. Sequence-specific cutoff values for abnormal native T1 and T2 values at 3-T were defined as >1,105 ms for T1 and >37.4 ms for T2, respectively. These were based on previously derived sequence-specific cutoffs of 2 SDs above the respective means in an independent cohort of subjects with no pre-existing conditions or regular medication (n = 85; male subjects, n = 51 [60%]; age [median (IQR)], 45 years [31 to 54 years]), using the exact same sequences and scanning equipment.

TABLE 2 Baseline Laboratory Markers and CMR Findings

	No CV Events (n = 132)	CV Events (n = 24)	p Value
Routine blood biomarkers			
Hemoglobin, mg/dl	15 (14–16)	14 (12–16)	0.33
eGFR, ml/min/1.73 m^2	84 (70–99)	79 (60–95)	0.30
hs-CRP, mg/l	0.15 (0.08–0.27)	0.2 (0.08–1.12)	0.08
hs-TnT, ng/l	5.0 (3.0–8.1)	6.0 (3.0–14.8)	0.20
NT-proBNP, pg/l	48 (23–82)	109 (25–337)	**0.003**
Functional and structural measures			
LV-EDVi, ml/m^2	83 (74–94)	94 (72–101)	0.13
LV mass index, g/m^2	57 (49–64)	65 (49–77)	0.04
LV EF, %	58 (54–62)	55 (49–64)	**0.052**
RV EF, %	56 (51–60)	55 (50–58)	0.61
LA area, cm^2	23 (20–26)	22 (18–24)	0.81
Tissue characterization			
Native T1, ms	1,110 (1,075–1,138)	1,149 (1,115–1,163)	**0.001**
Native T2, ms	37 (36–39)	40 (38–41)	**0.009**
Myocardial LGE present	24 (18)	11 (46)	**0.002**
Ischemic LGE	7 (5)	6 (25)	**<0.001**
Nonischemic LGE	17 (13)	5 (21)	0.30
LGE extent (% LV mass)	8.2 (6.0–10.7)	11.6 (7.9–12.1)	0.50
Significant ischemia	4 (3)	1 (4)	0.80

Values are median (interquartile range) or n (%). The **bold** p values <0.05 were considered significant.

CMR = cardiac magnetic resonance; CV = cardiovascular; hs-CRP = high sensitivity C-reactive protein; EDVI = end-diastolic volume index; eGFR = estimated glomerular filtration rate; hs-TnT = high-sensitivity troponin T; NT-proBNP = N-terminal pro-B-type natriuretic peptide; EF = ejection fraction; LA = left atrial; LGE = late gadolinium enhancement; LV = left ventricular; RV = right ventricular.

RESULTS

The baseline characteristics of the patient population are summarized in Tables 1 and 2. Datasets of 156 subjects (62% male subjects; age [median (IQR)]: 50 years [42 to 57 years]; CD4 count: 652 cells/μl [403 to 949 cells/μl]) were included in the final analysis. The median time from the original HIV diagnosis to the date of CMR was 10.4 years (3.8 to 17.2 years). All patients were on stable HAART a minimum of 6 weeks before the index CMR. Twenty-eight patients (18%) received treatment of dyslipidemia with statins. A single patient (0.7%) was lost to follow-up; 2 patients died of multiorgan failure due to sepsis. Patients with events were similar in age, sex, cardiovascular risk factors, and scores to those without events. Patients

TABLE 3 Results of Univariable and Multivariable Analyses in Prediction of the Cardiovascular Endpoint

Univariable Analyses	Hazard Ratio (95% CI)	p Value
Cardiovascular profile		
Age, yrs	0.85 (0.68–1.06)	0.15
Male	1.8 (0.78–5.50)	0.62
Smoking	0.84 (0.31–2.30)	0.84
Known HF	1.9 (0.54–6.90)	0.31
NYHA functional class ≥III	1.14 (0.4–3.3)	0.81
D:A:D 5 y (R) (lg10)	1.68 (0.43–6.46)	0.46
D:A:D 5 y (F) (lg10)	1.62 (0.52–5.13)	0.41
FRS 10 y (lg10)	2.4 (0.67–8.62)	0.18
MAGGIC (lg10)	1.7 (0.46–5.13)	0.23
Blood markers		
Hemoglobin (mg/dl)	0.79 (0.47–1.30)	0.37
NT-proBNP (lg10)	2.61 (1.42–4.80)	0.002
hs-TnT (lg10)	3.44 (1.31–9.07)	0.012
hs-CRP (lg10)	1.22 (0.53–2.82)	0.63
eGFR (lg10)	0.25 (0.01–10.21)	0.46
Imaging markers		
LV-EDVi, ml/m^2	1.02 (1.00–1.04)	0.02
LV mass index g/m^2	1.04 (1.01–1.07)	0.02
LVEF, %	0.94 (0.90–0.97)	0.001
Native T1, 10ms	1.19 (1.09–1.29)	<0.001
Native T2, ms	1.1 (0.99–1.23)	0.01
LGE present	2.4 (1.07–5.39)	0.03

Multivariable Analysis (Backward, Wald)	Variable	Hazard Ratio (95% CI), p Value
Chi-square (p value)		
15.9 (<0.001)	Native T1 (10 ms)	1.20 (1.08–1.33), 0.001
Model 2		
17.1 (<0.001)	Native T1 (10 ms)	1.17 (1.05–1.30), 0.007
	LV mass (g/m^2)	1.04 (1.00–1.07), 0.04

Multivariable analyses were performed with a backward (Wald) selection of variables; the thresholds for backward selection process in the model included p value of 0.05 for entry and 0.10 for removal of a variable. Adverse cardiovascular events included 4 HF deaths, 1 sudden cardiac death, 2 nonfatal acute myocardial infarction, 1 appropriate device discharge, and 16 HF hospitalizations. The p values for variables tested in the model (model 1, model 2) NT-proBNP (lg10; 0.33, 0.70), hs-TnT (lg10; 0.041, 0.69), LV EF (0.10, 0.48), LV EDVi (0.25, 0.72), LGE present (0.84, 0.52), and native T2 (0.26, 0.49).

Abbreviations as in Tables 1 and 2.

with events had higher native T1 (median [IQR]: 1,149 ms [1,115 to 1,163 ms] vs. 1,110 ms [1,075 to 1,138 ms]), native T2 (40 ms [38 to 41 ms] vs. 37 ms [36 to 39 ms]), LV mass index (65 g/m^2 [49 to 77 g/m^2] vs. 57 g/m^2 [49 to 64 g/m^2]) and NT-proBNP (109 pg/l [25 to 337 pg/l] vs. 48 pg/l [23 to 82 pg/l]) (all; $p < 0.05$). Participants with events had lower LV ejection fraction (median (IQR): 55% [49 to 64] vs. 58% [54 to 62]; $p = 0.052$). There was a significantly higher percentage of LGE among PLWH with events (46% vs. 18%; $p = 0.002$), with overall similar proportions of ischemic and nonischemic patterns in patients with events. A total of 5 patients had significant ischemia on myocardial perfusion imaging and underwent percutaneous coronary revascularization within 2 weeks from CMR.

During a median follow-up of 13 months (9 to 19 months), 24 adverse events were observed (4 HF deaths, 1 sudden cardiac death, 2 nonfatal acute myocardial infarction, 1 appropriate device discharge, and 16 HF hospitalizations) (Table 3). Baseline native T1 and T2, LV volumes, hs-TnT, and NT-proBNP were all significant univariable predictors of the primary endpoint. Respective Kaplan-Meier curves for imaging variables using binary cutoffs are shown in Figure 1. In multivariable analyses, native T1 was independently predictive of adverse events (chi-square test, 15.9; $p < 0.001$; native T1 [10 ms] HR (95% CI): 1.23 [1.11 to 1.35]; $p < 0.001$), followed by a model that also included LV mass (chi-square test, 17.1.00; $p < 0.001$; native T1 [10 ms] HR (95% CI): 1.17 [1.05 to 1.30]; $p = 0.007$; LV mass (g/m^2) HR [95% CI]: 1.04 [1.00 to 1.07]; $p = 0.04$). Traditional risk stratifiers (Framingham Risk Score, D:A:D, and MAGGIC score) or presence of ischemia on the baseline scan were not associated with the outcome events. Proportionally, more participants with events took non-nucleoside reverse transcriptase inhibitors ($p = 0.04$) and fewer used integrase inhibitors ($p = 0.021$). Two patients underwent endomyocardial biopsy based on CMR findings, revealing acute lymphocytic myocarditis and chronic borderline inflammatory changes, respectively (Figure 2).

DISCUSSION

The current study reports several important and novel observations. In a cohort of consecutive PLWH on stable long-term HAART, there was a 15% rate of adverse cardiovascular events in a short-term follow-up of 13 months. PLWH with and without adverse events were similar for baseline traditional risk factors and risk scores. Cardiac structural measures were on average only mildly abnormal. However, serum biomarkers, hs-TnT and NT-proBNP, as well as the myocardial tissue characteristics, native T1 and LGE, were all significantly associated with the events. Diffuse myocardial fibrosis and remodeling by native T1 mapping and LV mass were independently predictive of cardiovascular events. These findings together indicate a complex underlying pathophysiology in the development of heart disease in PLWH, with a prominent role of diffuse myocardial interstitial fibrosis in driving the clinical outcome. Our findings may support the development of novel personalized approaches to cardioprotection, including screening and anti-remodeling treatment in pre-HF, to reduce the HF burden in PLWH receiving long-term HAART.

FIGURE 1 Kaplan-Meier Curves for CMR Parameters and Cardiovascular Outcome

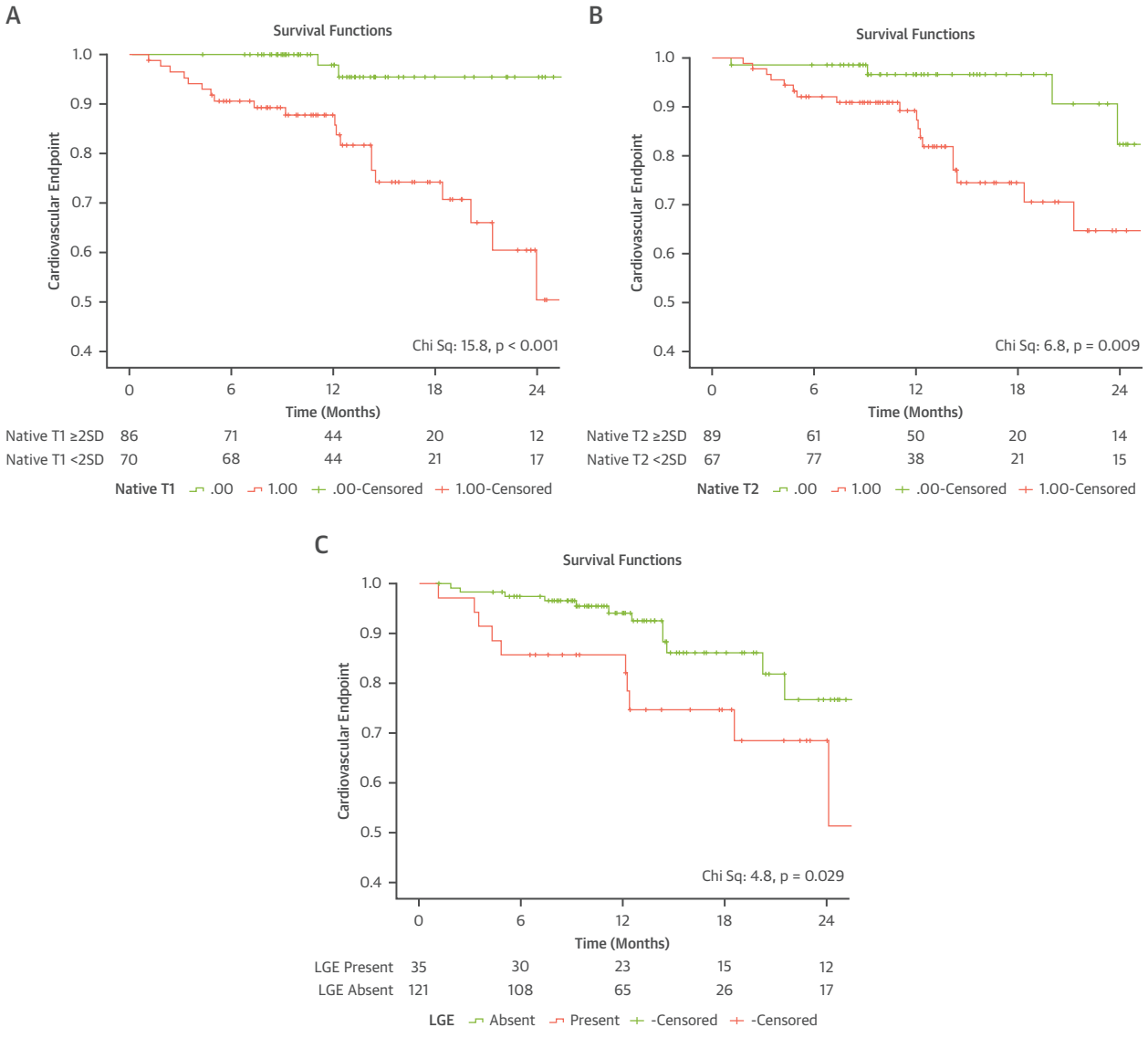

(A) Diffuse myocardial fibrosis by native T1 using Goethe CVI-modified Look-Locker imaging sequence (using a binary definition of 2 SDs above the mean of sequence-specific normal range of >1,105 ms for native T1 at 3-T). **(B)** Myocardial inflammation by native T2 (using a binary definition of 2 SDs above the mean of sequence-specific normal range; of >37.4 ms for native T2 at 3-T). **(C)** Myocardial scar by late gadolinium enhancement (LGE) (using a binary definition of present vs. absent LGE). CMR = cardiac magnetic resonance.

To the best of our knowledge, this study is the largest outcome trial to date in PLWH using CMR. A body of evidence previously highlighted detectable differences in blood biomarkers and cardiac imaging measures obtained in HIV-infected individuals compared with noninfected control subjects and related these with cardiovascular dysfunction and poor outcome (as reviewed elsewhere [29]). More recently, the role of inflammatory remodeling in addition to fibrosis by demonstrating elevated T1 mapping values was also put forward as an explanation for an increased incidence of HF in PLWH (3,7,29,30). Our current findings corroborate the previous observations regarding the prognostic role of the blood biomarkers and expand parallel investigations of the imaging markers, relating them comprehensively with short-term outcome. Our findings show that patients with events had more

FIGURE 2 Representative Case of a PLWH and Evidence of a Diffuse Inflammatory Myocardial Remodeling

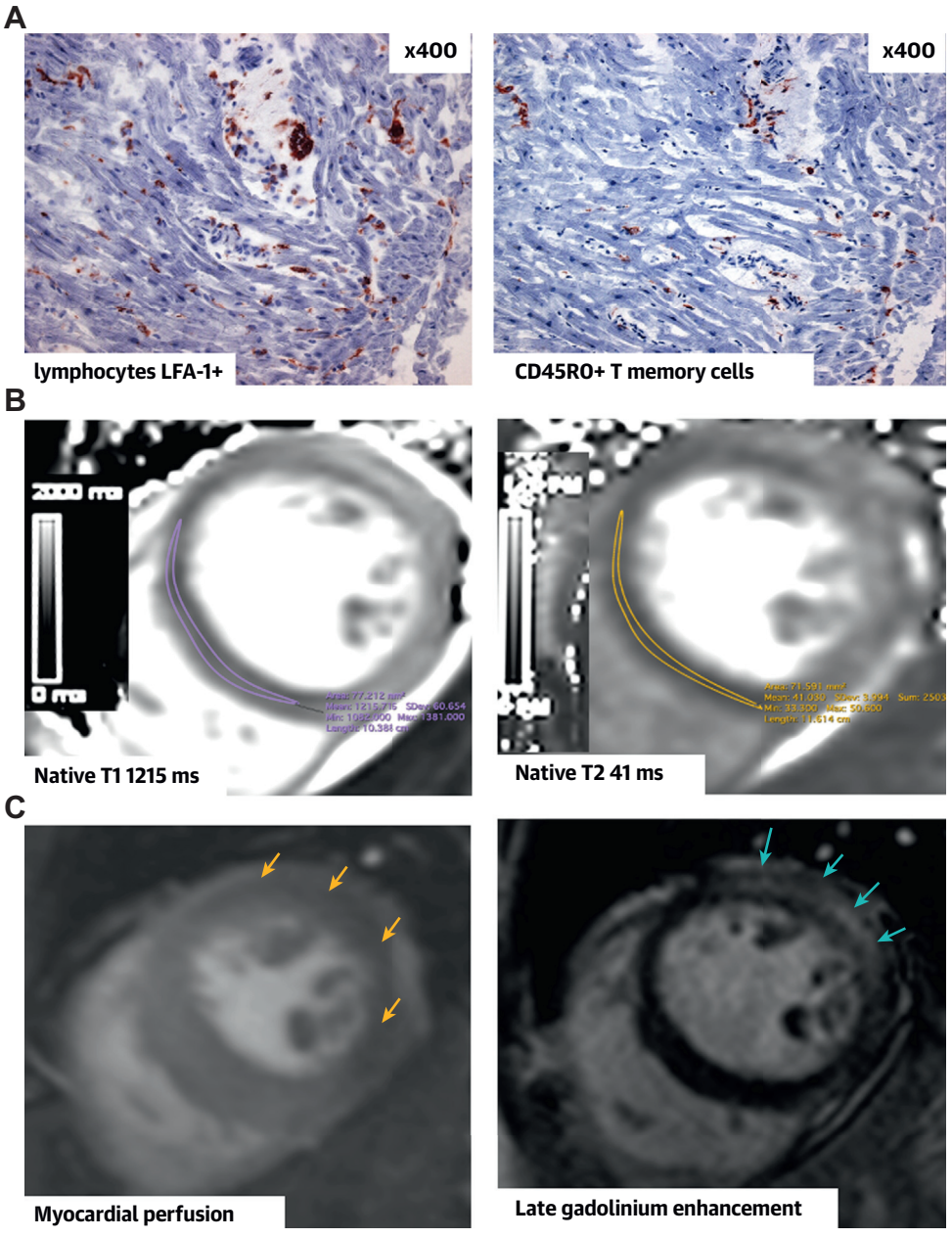

Endomyocardial biopsy panels reveal active lymphocytic myocarditis (lymphocytic markers: lymphocyte function associated antigen [LFA-1]; CD34RO lymphocyte T memory cells). Corresponding native T1 and T2 maps, myocardial perfusion, and late gadolinium enhancement images. Significantly raised native T1 and T2 in measurements by mid-ventricular septal sampling indicate diffuse fibrosis and inflammation. Myocardial perfusion and late gadolinium enhancement images reveal an area of hypoperfusion **(yellow arrowheads)** and scar **(blue arrowheads)** in lateral segments of the myocardium.

myocardial scar, although ischemic and nonischemic patterns were present in equal proportions. This finding suggests that ischemic heart disease is unlikely the sole pathophysiological driver of cardiac impairment. The disparity in diffuse processes of fibrosis and inflammation, measured in nonscarred myocardium by native T1 and T2, respectively, was proportionally even greater between patients with

CENTRAL ILLUSTRATION **Proposed Cardiovascular Care in People Living With Human Immunodeficiency Virus Supported by Cardiac Magnetic Resonance**

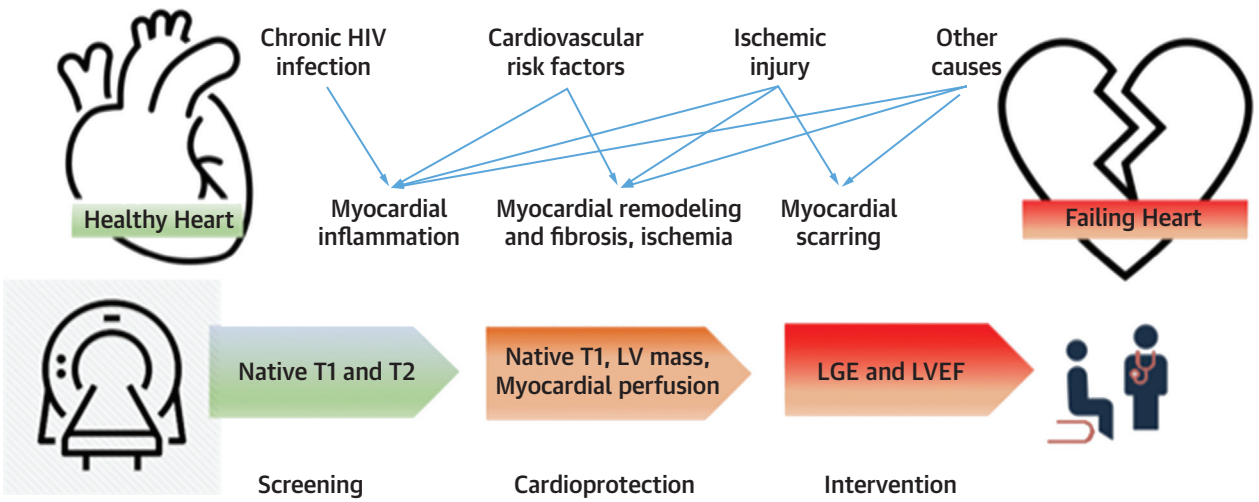

de Leuw, P. et al. J Am Coll Cardiol Img. 2021;14(8):1548–57.

Our results suggest that cardiac magnetic resonance (CMR) may provide a potentially helpful noninvasive tool to support personalized cardiovascular care in people living with human immunodeficiency virus (PLWH). This tool may help with screening for early inflammatory involvement, to cardioprotection by intensive cardiovascular risk factor management and anti-remodeling treatment, to therapeutic intervention in early heart failure, to reduce the overall burden of heart disease in PLWH on long-term antiretroviral therapy. LGE = late gadolinium enhancement; LV = left ventricular; LVEF = left ventricular ejection fraction.

and without events. This finding substantiates the hypothesis linking intrinsic myocardial inflammatory processes and HF complications in PLWH (3), as well as draws parallels with inflammatory cardiomyopathies, linking diffuse inflammation with structural heart remodeling and dysfunction, and prognostic association with worse cardiovascular outcome (18) (as summarized by Winau et al. [31]). Results of endomyocardial biopsy, performed in selected patients with imaging findings of active myocarditis (**Figure 2**), lend further support to this notion.

Cardiovascular outcomes in the current study were primarily composed of HF-related events, concordant with the notion that PLWH are more likely to develop HF compared with noninfected individuals (8). A previous study suggested a connection between an ongoing low-grade systemic inflammation and severity of LV dysfunction (7). Whereas patients with events had overall only relatively mild functional impairment, the univariate predictive association of measures of structural heart disease and blood biomarkers provide a pathophysiological parallel to this previous observation. Evidence suggests that HAART reduces the systemic inflammation in PLWH, and integrase inhibitors seem to reduce inflammation to a greater degree than the non-nucleoside reverse transcriptase inhibitors (32). Although we found that patients with events took fewer integrase inhibitors, this was only mildly significant and not predictive of events. Larger studies are required to verify this effect. In the current cohort, a minority of participants had evidence of previous ischemic heart disease, suggesting that individuals at risk of HF may be difficult to identify using population-derived risk scores, which specifically relate to the ischemic outcomes. This is also supported by the lack of predictive power of the D:A:D and the MAGGIC scores. Nevertheless, our findings lend support to the underlying pathophysiological commonality by linking myocardial inflammation, extracellular matrix remodeling, and fibrotic repair, which seem to be ongoing despite the stable HAART (Supplemental Figure 1S).

Troponin and NT-proBNP have both been predictive of outcome in univariate analyses, drawing parallels between the injury and HF; however, neither marker has surpassed the native T1 in predictive relationship, reiterating the high sensitivity of native T1 for detection of intrinsic myocardial pathology. As emphasis on identifying pre-HF stages is growing, our findings may inform the development of necessary approaches of personalized care in this population at risk, by screening for heart disease, guiding prevention, and intervention with anti-remodeling

treatment in early HF (**Central Illustration**). Whether intervention based on native T1 improves outcome must be assessed in a future study. Because CMR can inform on ischemic and nonischemic pathophysiological components, it is uniquely placed to capture the diverse underlying pathophysiology encountered in PLWH.

STUDY LIMITATIONS. A relatively small sample size and a composite endpoint are the major limitations of this study. Cardiovascular endpoints were ascertained by physician-based adjudication and biomarker results (7,8). Larger future studies are needed to reconfirm our findings and establish the benefit for the patient population in question. The participants were recruited from a single tertiary center with high-level, dedicated specialist care and unlimited access to a wide range of HAART medication. The differences observed in HAART between patients with and without events need to be reconfirmed in a bigger sample. Expanding future studies to less homogeneous cohorts is necessary to gain insights into factors that may affect cardiovascular outcomes in other settings. Biopsies were performed in selected patients, based on a number of clinical markers, indicating a high likelihood of clinically relevant myocarditis, and not CMR alone. Hence, it could not be performed in all patients. The Goethe CVI-MOLLI sequence used for T1 mapping has been rigorously validated and employed in numerous previous publications in single, multicenter, and multivendor settings using standardized protocols and quality assurance. This sequence is known to be uniquely T2 sensitive and influenced by magnetization transfer; the measurements are sensitive to detect inflammation-driven myocardial pathophysiology (31,33). Our findings, this sequence-specific normal and cutoff values, cannot be transferred to other T1-mapping sequences or vendor products as these strive for high T1 accuracy (34,35).

Taken together, our findings show that native T1 measured noninvasively by CMR is the strongest predictor of cardiovascular events, followed by a model that also included LV mass, together reflecting the pathological myocardial remodeling. Our results support that monitoring using CMR is a potentially helpful noninvasive tool without radiation for the development of novel approaches to cardioprotection, with the goal of reducing the burden of HF in PLWH and long-term antiretroviral therapy.

ACKNOWLEDGMENTS The authors thank their supporting staff for the dedicated hard work. This work is a tribute to a patient-centered multidisciplinary care between colleagues, imagers, cardiologists, radiologists, and infectious disease specialists.

FUNDING SUPPORT AND AUTHOR DISCLOSURES

This study was supported by the German Ministry of Education and Research via the German Centre for Cardiovascular Research (DZHK) to Drs. Puntmann, Zeiher, and Nagel. The authors have reported that they have no relationships relevant to the contents of this paper to disclose.

ADDRESS FOR CORRESPONDENCE: Dr. Valentina O. Puntmann, Institute of Experimental and Translational Cardiac Imaging, DZHK Centre for Cardiovascular Imaging, Theodor-Stern Kai 7, University Hospital Frankfurt, 60590 Frankfurt am Main, Germany. E-mail: vppapers@icloud.com.

PERSPECTIVES

COMPETENCY IN MEDICAL KNOWLEDGE: PLWH have increased risk of HF compared with the noninfected population. In addition to traditional cardiovascular risk factors or atherosclerotic complications, diffuse myocardial inflammation and fibrosis have been proposed to play a role in the underlying pathophysiological remodeling.

TRANSLATIONAL OUTLOOK: CMR provides insights into diverse pathways of pathological myocardial remodeling. Native T1 measured noninvasively by CMR is the strongest predictor of cardiovascular events, followed by a model with LV mass, together reflecting the pathological myocardial remodeling. These findings may inform personalized approaches to screening and early intervention to reduce the burden of heart failure.

REFERENCES

1. Shah ASV, Stelzle D, Lee KK, et al. Global burden of atherosclerotic cardiovascular disease in people living with HIV. *Circulation*. 2018;138:1100–1112.

2. Alonso A, Barnes AE, Guest JL, Shah A, Shao IY, Marconi V. HIV Infection and incidence of cardiovascular diseases: an analysis of a large healthcare database. *J Am Heart Assoc*. 2019;8:3.

3. Hsue PY, Tawakol A. Inflammation and fibrosis in HIV. *Circ Cardiovasc Imaging*. 2016;9:737.

4. Butler J, Kalogeropoulos AP, Anstrom KJ, et al. Diastolic dysfunction in individuals with human immunodeficiency virus infection: literature review, rationale and design of the Characterizing Heart Function on Antiretroviral Therapy (CHART) Study. *J Cardiac Fail*. 2018;24:255–265.

5. Ntusi N, O'Dwyer E, Dorrell L, et al. HIV-1–related cardiovascular disease is associated with

chronic inflammation, frequent pericardial effusions, and probable myocardial edema. *Circ Cardiovasc Imaging*. 2016;9:560.

6. Holloway CJ, Ntusi N, Suttie J, et al. Comprehensive cardiac magnetic resonance imaging and spectroscopy reveal a high burden of myocardial disease in HIV patients. *Circulation*. 2013;128:814–822.

7. Freiberg MS, Chang CCH, Skanderson M, et al. Association between HIV infection and the risk of heart failure with reduced ejection fraction and preserved ejection fraction in the antiretroviral therapy era. *JAMA Cardiol*. 2017;2:536.

8. Feinstein MJ, Steverson AB, Ning H, et al. Adjudicated heart failure in HIV-infected and uninfected men and women. *J Am Heart Assoc*. 2018;7:737.

9. Piepoli MF, Hoes AW, Agewall S, et al. 2016 European guidelines on cardiovascular disease prevention in clinical practice. *Eur Heart J*. 2016;37:2315–2381.

10. Ryom L, Cotter A, De Miguel R, et al. 2019 update of the European AIDS Clinical Society Guidelines for treatment of people living with HIV version 10.0. *HIV Med*. 2020;21:617–624.

11. Gadolinium-containing contrast agents. Available at: https://www.ema.europa.eu/en/medicines/human/referrals/gadolinium-containing-contrast-agents-0 https://www.fda.gov/drugs/postmarket-drug-safety-information-patients-and-providers/information-gadolinium-based-contrast-agents https://www.acr.org/Clinical-Resources/Contrast-Manual. Last accessed September 10, 2020.

12. Congestive Heart Failure. Available at: https://www.framinghamheartstudy.org/fhs-risk-functions/congestive-heart-failure/. Last accessed September 10, 2020.

13. Friis-Møller N, Thiébaut R, Reiss P, et al. Predicting the risk of cardiovascular disease in HIV-infected patients: the data collection on Adverse Effects of Anti-HIV Drugs Study. *Eur J Cardiovasc Prevent Rehabil*. 2010;17:491–501.

14. Pocock SJ, Ariti CA, McMurray JJV, et al. Predicting survival in heart failure: a risk score based on 39 372 patients from 30 studies. *Eur Heart J*. 2012;34:1404–1413.

15. Kramer CM, Barkhausen J, Bucciarelli-Ducci C, Flamm SD, Kim RJ, Nagel E. Standardized cardiovascular magnetic resonance imaging (CMR) protocols: 2020 update. *J Cardiovasc Magnetic Resonance*. 2020;22:17–18.

16. Child N, Suna G, Dabir D, et al. Comparison of MOLLI, shMOLLLI, and SASHA in discrimination between health and disease and relationship with histologically derived collagen volume fraction. *Eur Heart J Cardiovasc Imaging*. 2017;19:768–776.

17. Puntmann VO, Carr-White G, Jabbour A, et al. T1-mapping and outcome in nonischemic cardiomyopathy. *J Am Coll Cardiol Img*. 2016;9:40–50.

18. Puntmann VO, Carr-White G, Jabbour A, et al. Native T1 and ECV of noninfarcted myocardium and outcome in patients with coronary artery disease. *J Am Coll Cardiol*. 2018;71:766–778.

19. Fernández-Jiménez R, Sánchez-González J, Agüero J, et al. Fast T2 gradient-spin-echo (T2-GraSE) mapping for myocardial edema quantification: first in vivo validation in a porcine model of ischemia/reperfusion. *J Cardiovasc Magn Reson*. 2015;17:652.

20. Giri S, Chung YC, Merchant A, et al. T2 quantification for improved detection of myocardial edema. *J Cardiovasc Magn Reson*. 2009;11:56.

21. Schulz-Menger J, Bluemke DA, Bremerich J, et al. Standardized image interpretation and post-processing in cardiovascular magnetic resonance—2020 update: Society for Cardiovascular Magnetic Resonance (SCMR): Board of Trustees Task Force on Standardized Post-Processing. *J Cardiovasc Magn Reson*. 2020;22:19–22.

22. Rogers T, Dabir D, Mahmoud I, et al. Standardization of T1 measurements with MOLLI in differentiation between health and disease—the ConSept study. *J Cardiovasc Magn Reson*. 2013;15:78.

23. Dabir D, Child N, Kalra A, et al. Reference values for healthy human myocardium using a T1 mapping methodology: results from the international T1 multicenter cardiovascular magnetic resonance study. *J Cardiovasc Magn Reson*. 2014;16:34.

24. Nagel E, Greenwood JP, McCann GP, et al. Magnetic resonance perfusion or fractional flow reserve in coronary disease. *N Engl J Med*. 2019;380:2418–2428.

25. Le MTP, Zarinabad N, D'Angelo T, et al. Subsegmental quantification of single (stress)-pass perfusion CMR improves the diagnostic accuracy for detection of obstructive coronary artery disease. *J Cardiovasc Magn Reson*. 2020;22:14.

26. Hicks KA, Tcheng JE, Bozkurt B, et al. 2014 ACC/AHA key data elements and definitions for cardiovascular endpoint events in clinical trials. *J Am Coll Cardiol*. 2015;66:403–469.

27. Jaffe AS, Morrow DA, ESC Scientific Document Group, et al. Fourth universal definition of myocardial infarction (2018). *Eur Heart J*. 2018;40:237–269.

28. Ponikowski P, Voors AA, Anker SD, et al. 2016 ESC guidelines for the diagnosis and treatment of acute and chronic heart failure. *Eur Heart J*. 2016;37:2129–2200.

29. Hsue PY, Waters DD. Time to recognize HIV infection as a major cardiovascular risk factor. *Circulation*. 2018;138:1113–1115.

30. Alvi RM, Afshar M, Neilan AM, et al. Heart failure and adverse heart failure outcomes among persons living with HIV in a US tertiary medical center. *Am Heart J*. 2019;210:39–48.

31. Winau L, Hinojar Baydes R, Braner A, et al. High-sensitive troponin is associated with subclinical imaging biosignature of inflammatory cardiovascular involvement in systemic lupus erythematosus. *Ann Rheumatic Dis*. 2018;77:1590–1598.

32. Hileman CO, Funderburg NT. Inflammation, immune activation, and antiretroviral therapy in HIV. *Curr HIV/AIDS Rep*. 2017;14:93–100.

33. Puntmann VO, Carerj ML, Wieters I, et al. Outcomes of cardiovascular magnetic resonance imaging in patients recently recovered from coronavirus disease 2019 (COVID-19). *JAMA Cardiol*. 2020;5:1265–1273.

34. Robson MD, Piechnik SK, Tunnicliffe EM, Neubauer S. T1 measurements in the human myocardium: the effects of magnetization transfer on the SASHA and MOLLI sequences. *Magn Reson Med*. 2013;70:664–670.

35. Kellman P, Hansen MS. T1-mapping in the heart: accuracy and precision. *J Cardiovasc Magn Reson*. 2014;16:92.

KEY WORDS cardiac magnetic resonance, myocardial fibrosis, scar

APPENDIX For sequence parameters, postprocessing and interpretation, and post hoc analysis, please see the online version of this paper.